



SB-4

**THE DEVELOPMENT OF THE DENSE INSTRUMENT ARRAY SYSTEM 'KASSEM'
AND
THE ANALYSIS OF OBSERVED EARTHQUAKE WAVES**

Teruo SHIMIZU¹, Ken'ichi ABE¹, Kin'ichi KASUDA¹,
and Eiji YANAGISAWA²

¹Nuclear Energy Development Division, KUMAGAI-GUMI Co., LTD
2-1 Tsukudo-cho, Shinjuku-ku, Tokyo, Japan

²Department of Civil Engineering, Tohoku University
Aoba, Aramaki Sendai-shi, Miyagi, Japan

SUMMARY

As Earthquake proof design is more in advance, it is especially important to observe strong ground motion by instrument array method. The authors have developed a strong motion earthquake instrument array in order to investigate mainly the wave propagation in the ground and deployed to the typical geology in Japan consisting of granitic formation, soft rockformation, diluvium and alluvium. This paper deals with the summary of this instrument array system and the analysis of the observed waves.

INTRODUCTION

Strong motion earthquake instrument array was recommended in the International Workshop of IABE (1979.5). Therefore, some of large instrument arrays have been deployed in Japan. Most of observation systems can be classified into elemental array and special array, and they are intended for near field and soil-structure interaction studies rather than far field ones. Considering future earthquake proof design, it will become especially important to grasp the wave propagation in the ground. Therefore, observation by dense instrument array is exceedingly effective to make clear the characteristics of seismic ground motion.

Taking into account of the above situations, main objectives of planned observation are;

(1) to obtain ground vibration and response data on granite, soft rock, diluvium and alluvium (2) to investigate the three dimensionally wave propagation in consideration of ground structure. (3) to make basic data for simulating the seismic ground motion from the fault information and vibration characteristics of ground included in the basement rock records(4) to investigate on liquefaction by monitoring transient changes in pore pressure.

This array system installed for these purposes has been arranged along the coastal area in Miyagi and Fukushima prefs. and is called KASSEM(:KUMAGAI-GUMI ARRAY SYSTEM FOR STRONG EARTHQUAKE MOTION) consisting of both local laboratory array and simple extended array. This paper deals with the summary of KASEEM and the analysis of observation waves from local laboratory array and simple extended array.

SUMMARY OF KASSEM

The main features of KASSEM can be summarized as follows, describing the deployment of seismographs, the in-site investigation and the instrument system

Deployment of Seismographs KASSEM covers partially one of the Specified observation areas in Japan as shown in Fig.1. The Center Array (C.A), the heart of KASSEM, is located in Shibata-cho, Miyagi pref. and consists of local laboratory array with three dimensional deployment on and under the ground. There is another type of array in KASSEM. The seismograph are arranged on the surface of the ground to cover the coastal area of Miyagi and Fukushima prefs. This array is called Strong Motion Array(S.M.A) making up for the C.A and forms simple extended array with C.A.

The purpose of C.A is to investigate the nature of wave propagation on and under the ground consisting of horizontal layers; namely granite, soft rock, diluvium and alluvium. As Fig.2, 12 triaxial velocity seismographs of borehole-type are arranged three dimensionally and this array consists of the tripartite array which length of a side is about 400m and the vertical array extended from the ground surface to the depth of about 400m in the center of this tripartite array. Each velocity seismographs is set up on the ground surface and soft rock at each vertex of tripartite array and in the different layers at the center of this array as follows; namely on and in the middle of alluvium, diluvium and soft rock, and on granite respectively. Triaxial accelerographs buried at the points of soft rock (V4) and granite(V6). Three piezometers are additionally placed at three points from the depth of H1 to H2.

S.M.A enables us to catch the change of earthquake waves propagating to C.A site because each triaxial accelerograph is provided at the changing points of topography and geological structure. Each observation point in S.M.A array covers wide area as shown in Fig.1 and forms several large tripartite arrays.

Overall amplitude and phase response of seismograph to be used is given in Fig.3.

Ground Investigation Extensive site investigation and laboratory tests were carried out in order to evaluate the material properties and the geological structure where KASSEM was installed. Especially two boreholes for exploration were excavated at C.A site. Detailed in-situ investigation using the boreholes and laboratory tests were carried out. As a result of these investigations the cross section as shown in Fig.4 can be estimated. This cross section shows geological features near the C.A site between No2- No4 observation points.

In addition, the soil profiles at C.A site are obtained as shown in Fig.5 and the material propertie were determined. Dynamic properties of soft rock were shown as Fig.6.

Digital Seismic Data Acquisition System Fig.7 shows a schematic diagram of the recording and processing system. The trigger level of C.A. recorder is adjusted at 0.05 kine. All measurements are simultaneously started when one of the vertical and horizontal signals exceeds the preset level at H6 instrument.

Detected signals on the earthquake are converted into digital values of 16-bit words at every 0.005 second, making use of A/D converter at manholes in the subsurface (points H and V). Then, they are sent to the observatory by the digital electrical transmitter and are recorded on a magnetic tape. Each device has a digital memory for a 10.24 sec time delay, to record not only the S-wave but also P-wave information, and has time code generator to be corrected every day with accuracy to 1/100 sec by the time signal from NHK

broadcast.

Although SAMTAC-17S used in S.M.A. by itself has the similar recording process function to C.A., its delay time is 5.12 sec and each datum recorded on the digital cassette tape is edited to match the C.A. data format through data converter. Therefore, all data channels are synchronized for a common time base and are collectively processed by the computer (ACOS-850).

THE ANALYSIS OF RECORDED WAVES

During four years observation from 1984 to 1987 KASSEM has recorded about 90 earthquakes with magnitude between 3.5 and 6.7. These location of epicenters and magnitudes are illustrated in Fig.1.

We will describe the characteristics of earthquake waves recorded at the C.A point and the S.M.A points surrounding C.A.

Besides, the analysis of pore pressure have been sammarized in Technical session D10-03 of 9th WCBE.

Characteristic of Cecter Array Records A total of 30 events was obtained at C.A site. Fig.8 shows amplification ratio of maximum values (velocity) along the vertical array points in C.A. Compared with vertical component, the amplification ratio of horizontal ones tends to increase in alluvium and diluvium layers and these value become 7~8 times of average value at V6 point (GL-401m), but in the lower part of V4 point deep hardly increases.

In order to estimate the amplification ratios of multilayers, velocity response spectra on recorded waves at each vertical array point were analyzed by the multiple regression method. The multiple regression equation used in this study is as follows.

$$\log_{10} V(T) = a(T)M_J^2 + b(T)M_J - c(T)\log_{10}(\Delta + 30) - e(T)D - d(T) + \sum_{i=1}^{N-1} (A_i(T) + B_i(T)V)S_i \quad (1)$$

where $V(T)$, M_J , Δ and D are the response spectrum amplitude, magnitude, epicentral distance (Km) and hypocentral depth (Km) respectively.

$a(T)$, $b(T)$, $c(T)$, $d(T)$, $e(T)$, $A_i(T)$, $B_i(T)$, are their regression coefficients and T is period. Furthermore, $S_i (i=1, 2, \dots, N)$ are dummy variables. Based on the result of regression analysis, the change of amplification spectrum along the vertical array in C.A was examined. The recorded wave on 4/23 in 1987 $M_J = 6.5$, $\Delta = 123$ was selected as an example. The amplification ratio of this wave is obtained by one dimensional wave propagation theory as shown in Fig.9 and the result of regression analysis on $M_J = 6.5$ and $\Delta = 123$ is shown in Fig.10. As compared both amplification ratio, the tendency of amplification coincided.

Calculating the nonstationary spectra of most recorded waves in C.A by means of multi-filtering, the dispersion appears around the predominant periodon the response spectrum. Assuming that the wave propagate horizontally from its epicenter, the phase velocity is obtained by using tripartite array as shown in Fig.11 and Fig.12 (Recorded wave on 2/6 in 1987, $M_J = 6.7$, $\Delta = 156$). Each figure shows that the velocity increases as the period becomes longer and that the estimated phase velocities comparatively agree with the theoretical curve. It seems that surface waves appear in the surface layer at C.A site. However, it is difficult to separate surface waves, because such geological structure of C.A tends to generate various kind of waves around the predominant period as a result of theoretical amplification analysis on SH, SV, Rayleigh and Love wave.

Characteristics of Strong Motion Array Record One of the important features of KASSEM is that the seismographs are arranged at both locations on the

outcrop and in the same formation. Recorded waves on and in granite formation were examined. The maximum amplitude on horizontal components became about two times at the point on the outcrop and the amplification of velocity response spectra on the outcrop becomes several times in periods shorter than 0.3 sec. As an example the time history and nonstationary spectra on velocity are shown in Fig.13 (Recorded wave on 4/23 in 1987). It is noted that a peak value with the nature of dispersion exists in the period longer than 1.5 sec and their wave shape are similar. Especially the particle orbits obtained by these waves showed good agreement between these points on 1.5 sec longer.

In addition, the same regression analysis for S.M.A records at each point was carried out, provided that V was ignored in equation (1). The amplification spectrum $10^{A_i(T)}$ on each S.M.A point are given in Fig.14 and the tendency of response spectrum on each point was clearly explained.

CONCLUSION

The array observation system KASSEM has been developed and the observation is still continuing. In an attempt to obtain earthquake ground motions and in-situ pore pressure records, KASSEM's effectiveness has been confirmed. Furthermore, the characteristics of amplification, propagation and local ground influence in KASSEM site have been revealed through various analysis.

REFERENCES

1. Wilfred D. Iwan, "The deployment of strong-motion earthquake instrument arrays", Earthquake engineering and structural dynamics, Vol. 7, 413-426, (1979)
2. T. Shimizu, et al., "Summary of Kumagai Gumi array system for strong earthquake motion (in Japanese), Kumagai technical research report No36, 85-96, (1985)
3. M. Kamiyama; "Source characteristics inferred from the statistically analyzed spectra of strong motions with aid of dynamic model of faulting, Proc. of JSCE, (1987).

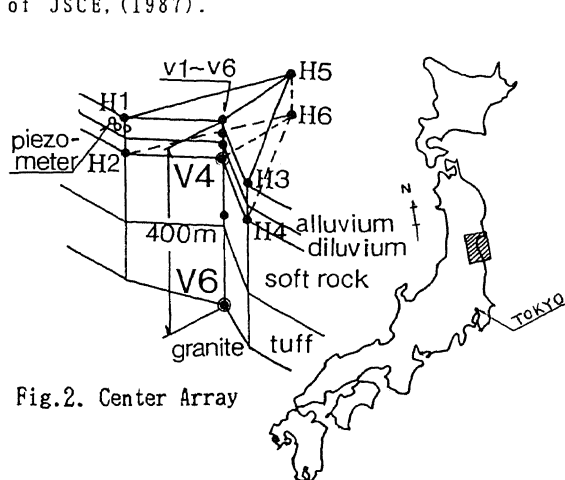


Fig.2. Center Array

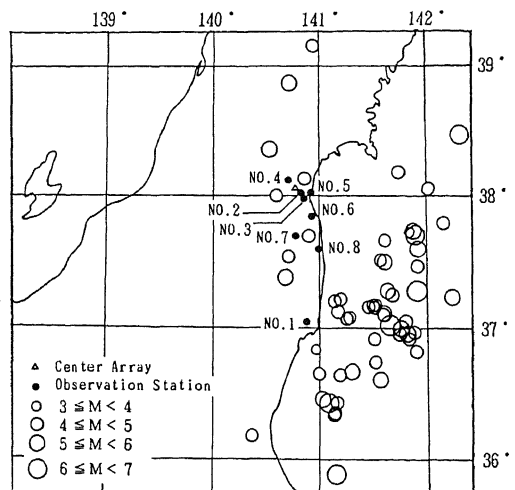


Fig.1. Location of seismometer and recorded earthquakes

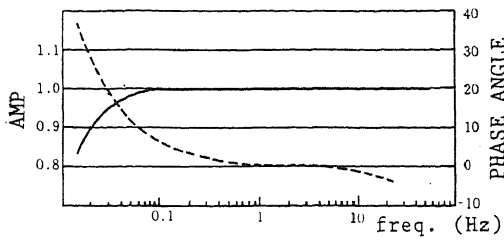


Fig.3(a) Frequency characteristics of a velocity seismograph

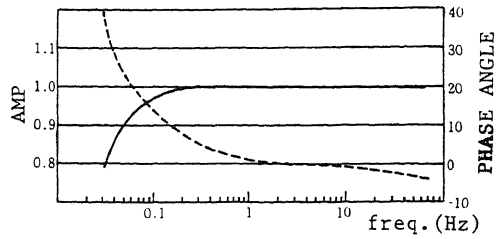


Fig.3(b) Frequency characteristic of an accelerograph

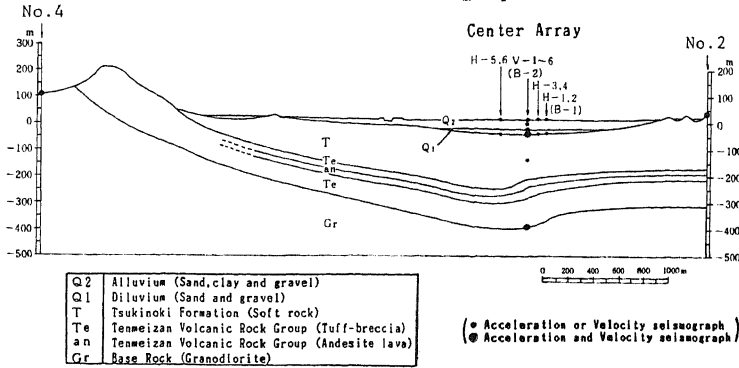


Fig.4 Cross section through No.2 - No.4 seismographs

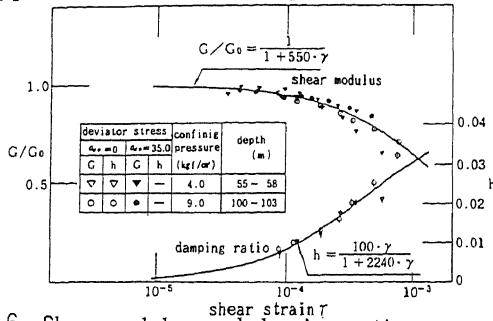


Fig.6. Shear modulus and damping ratio versus shear strain for soft rock

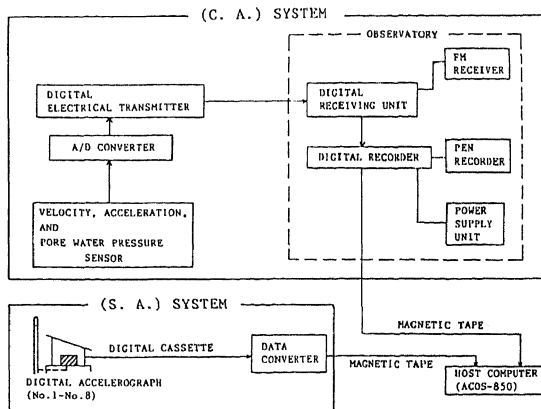


Fig.7. Schematic diagram of recording and processing system

Seismo-graph	Depth (m)	Geology	P-wave velocity (km/sec)					Unit weight (t/m ³)
			1	2	3	4	5	
V-1	0							1.65
V-2	-20	Q2						1.46
V-3	-34							1.53
V-4	-54	Q1						1.81
	-80							2.00
V-5	-220	T						2.07
	-255	Te						2.24
	-295	an						2.54
	-325							2.24
	-360	Te						2.26
V-6	-395	Gr						2.23
								2.34

Fig.5. Soil profile at Center Array (V1-V6)

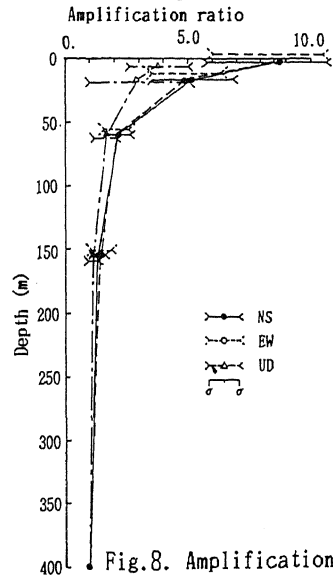


Fig.8. Amplification ratio of maximum values

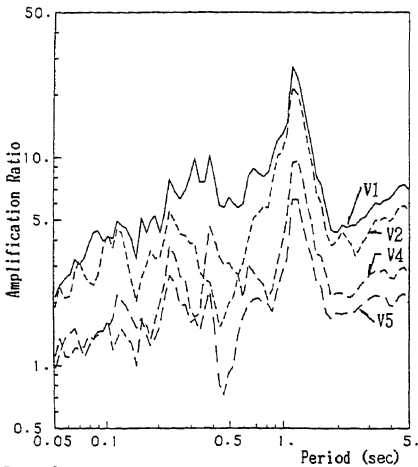


Fig.9. Amplification ratio obtained by one-dimensional wave propagation theory

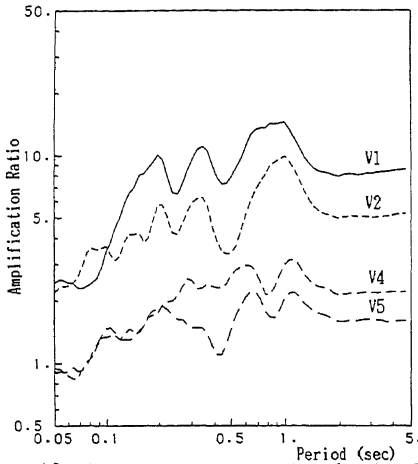


Fig.10. Amplification ratio obtained by multiple regression analysis

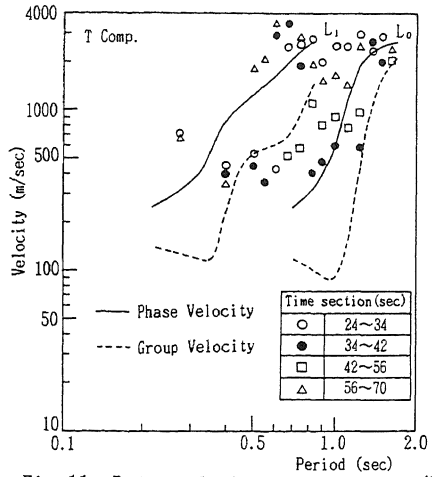


Fig.11. Detected phase velocities (T Comp.) and dispersion curve for Love wave

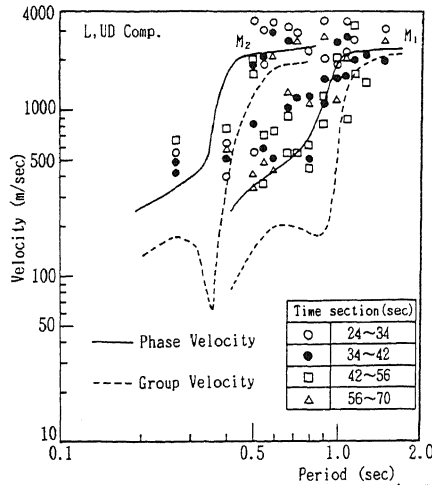


Fig.12. Detected phase velocities (L, UD Comp.) and dispersion curve for Rayleigh wave

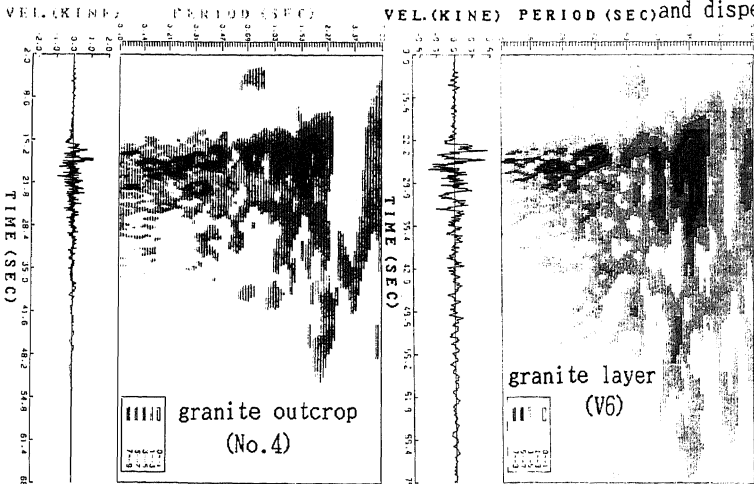


Fig.13. Non-stationary velocity spectra (T comp.)

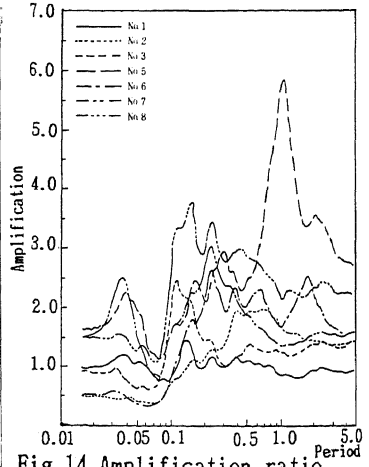


Fig.14. Amplification ratio of each S.M.A point to No.4